

Cranial Architecture of Tube-Snouted Gasterosteiformes (*Syngnathus rostellatus* and *Hippocampus capensis*)

Heleen Leysen,^{1*} Philippe Jouk,² Marleen Brunain,¹ Joachim Christiaens,¹ and Dominique Adriaens¹

¹Research Group Evolutionary Morphology of Vertebrates, Ghent University, Ghent, Belgium

²Royal Zool, Society of Antwerp, Antwerpen, Belgium

ABSTRACT The long snout of pipefishes and seahorses (Syngnathidae, Gasterosteiformes) is formed as an elongation of the ethmoid region. This is in contrast to many other teleosts with elongate snouts (e.g., butterflyfishes) in which the snout is formed as an extension of the jaws. Syngnathid fishes perform very fast suction feeding, accomplished by powerful neurocranial elevation and hyoid retraction. Clearly, suction through a long and narrow tube and its hydrodynamic implications can be expected to require certain adaptations in the cranium, especially in musculoskeletal elements of the feeding apparatus. Not much is known about which skeletal elements actually support the snout and what the effect of elongation is on related structures. Here, we give a detailed morphological description of the cartilaginous and bony feeding apparatus in both juvenile and adult *Syngnathus rostellatus* and *Hippocampus capensis*. Our results are compared with previous morphological studies of a generalized teleost, *Gasterosteus aculeatus*. We found that the ethmoid region is elongated early during development, with the ethmoid plate, the hyosymplectic, and the basihyal cartilage being extended in the chondrocranium. In the juveniles of both species almost all bones are forming, although only as a very thin layer. The elongation of the vomeral, mesethmoid, quadrate, metapterygoid, symplectic, and preopercular bones is already present. Probably, because of the long and specialized parental care which releases advanced developmental stages from the brooding pouch, morphology of the feeding apparatus of juveniles is already very similar to that of the adults. We describe morphological features related to snout elongation that may be considered adaptations for suction feeding; e.g. the peculiar shape of the interhyal bone and its saddle-shaped articulation with the posterior ceratohyal bone might aid in explosive hyoid retraction by reducing the risk of hyoid dislocation. *J. Morphol.* 271:255–270, 2010. © 2009 Wiley-Liss, Inc.

KEY WORDS: syngnathidae; cranial morphology; snout elongation; suction feeding

INTRODUCTION

The family Syngnathidae (Gasterosteiformes) encompasses the pipefishes and seahorses. Apart from the prehensile seahorse tail and the elongated pipefish body, syngnathids are characterized by their remarkably elongate snout (i.e., the part

of the head in front of the eyes). Unlike other long-snouted teleosts (e.g., butterflyfishes, Chaetodontidae), the tubular snout of syngnathids is not formed by the extension of the jaws, but by an elongation of the region between the autopalatine bone and the lateral ethmoid bone, namely the ethmoid region.

Pipefishes and seahorses approach their prey from below and a rapid neurocranial elevation positions the mouth close to the prey. Next, an explosive expansion of the snout followed by lower jaw depression cause water to flow into the mouth aperture (Muller and Osse, 1984; Muller, 1987; de Lussanet and Muller, 2007; Roos et al., 2009). Suction feeding in pipefishes and seahorses is the fastest ever recorded in teleosts. Muller and Osse (1984) found that *Entelurus aequoreus* captured its prey in 5 ms, whereas Bergert and Wainwright (1997) recorded a time of 5.8 ms for *Hippocampus erectus* and 7.9 ms for *Syngnathus floridae*. De Lussanet and Muller (2007) recorded capture times of 6–8 ms for *S. acus* and Roos et al. (2009) recorded 5.77 ms for *H. reidi*. It was recently discovered that newborns are even faster (Van Wassenbergh et al., 2009). However, having a long and narrow snout is not without hydrodynamic costs. For example, by increasing the length of the snout the moment of inertia increases. Secondly, it implies that a large difference in pressure between the buccal cavity and the surrounding water must be created (Poiseuille's law). Finally, as the upper and lower jaws closing the mouth aperture are minute, the prey size is constrained. Hence, the hydrodynamic implications of suction feeding through a long, narrow tube can be expected to rely on special adaptations in the feeding apparatus,

*Correspondence to: Heleen Leysen, Research Group Evolutionary Morphology of Vertebrates, Ghent University, K.L. Ledeganckstraat 35, B-9000 Ghent, Belgium. E-mail: heleen.leysen@UGent.be

Received 4 March 2009; Revised 5 August 2009; Accepted 5 August 2009

Published online 1 October 2009 in Wiley InterScience (www.interscience.wiley.com) DOI: 10.1002/jmor.10795

TABLE 1. List of specimens studied

| Species | UGMD no. | SL (mm) | HL (mm) | Age | Preparation |
|-------------------------------|----------|-------------------|---------|-----------|-------------|
| <i>Syngnathus rostellatus</i> | 175380 | 126.2 | 14.8 | Adult | AR |
| <i>Syngnathus rostellatus</i> | 175381 | 111.1 | 14.5 | Adult | AR |
| <i>Syngnathus rostellatus</i> | 175382 | 97.9 | 12.2 | Adult | AR & AB |
| <i>Syngnathus rostellatus</i> | 175383 | 105.0 | 13.0 | Adult | AR |
| <i>Syngnathus rostellatus</i> | 175384 | 11.0 | 1.8 | PrR | AR |
| <i>Syngnathus rostellatus</i> | 175385 | 14.5 | 2.3 | PrR | AR |
| <i>Syngnathus rostellatus</i> | 175386 | 11.3 | 2.2 | PrR | AR |
| <i>Syngnathus rostellatus</i> | 175387 | 11.4 | 1.9 | PrR | AR |
| <i>Syngnathus rostellatus</i> | 175388 | 13.1 ^a | 2.1 | PrR | SS |
| <i>Hippocampus capensis</i> | 175389 | 96.1 | 15.2 | Adult | AR |
| <i>Hippocampus capensis</i> | 175390 | 97.6 | 17.7 | Adult | AR |
| <i>Hippocampus capensis</i> | 175391 | 99.0 | 16.0 | Adult | AR |
| <i>Hippocampus capensis</i> | 175392 | 13.3 | 2.8 | 1 day PR | AR |
| <i>Hippocampus capensis</i> | 175393 | 13.6 | 2.9 | 2 days PR | AR & AB |
| <i>Hippocampus capensis</i> | 175394 | 12.8 | 2.8 | 3 days PR | SS |
| <i>Hippocampus capensis</i> | 175395 | 14.0 | 3.2 | 4 days PR | AR |
| <i>Hippocampus reidi</i> | 175396 | 117.2 | 23.8 | Adult | AR |
| <i>Hippocampus reidi</i> | 175397 | 113.5 | 21.4 | Adult | AR |
| <i>Hippocampus reidi</i> | 175398 | 7.01 | 1.9 | 1 day PR | SS |

Standard length of seahorses was measured as the sum of head length, trunk length, and tail length, according to the protocol by Lourie et al. (1999).

AB, alcian blue staining; AR, alizarin red staining; HL, head length; PrR, pre-release from brooding pouch; PR, post-release from brooding pouch; SL, standard length; SS, serial sectioning; UGMD, Zoological Museum of the Ghent University.

^aStandard length was estimated by interpolation based on the head length over standard length ratio of the other specimens.

particularly of musculoskeletal components forming and acting upon the jaws and ethmoid region.

To understand to what degree structural specializations of the tubular snout can be related to this highly performant suction feeding, a detailed examination of the morphology is needed. Thus far, studies dealing with syngnathid morphology are scarce or lack great detail (Branch, 1966; De Beer, 1937; Kadam, 1958, 1961; McMurrich, 1883). To fill this gap in current knowledge, this study focuses on the detailed anatomy of the cranial skeletal system of *Syngnathus rostellatus* (Nilsen's pipefish) and *Hippocampus capensis* (Knysna seahorse). Special attention is paid to the snout morphology to understand which skeletal elements are in fact elongated and what effect this elongation may have on the cranial architecture. The study of juveniles is required for a better comprehension of interspecific differences, as well as the detailed anatomical nature of snout elongation. The highly derived syngnathid morphology is compared with that of a generalized teleost, namely *Gasterosteus aculeatus* (three spined stickleback), both percomorph representatives, based on the study of Anker (1974).

MATERIALS AND METHODS

Four adults and five juveniles of *Syngnathus rostellatus*, three adults and four juveniles of *Hippocampus capensis* and two adults and one juvenile of *H. reidi* were studied (Table 1). The specimens of *S. rostellatus* were caught on the Belgian continental shelf (North Sea), whereas the specimens of *H. capensis* and *H. reidi* were obtained from the breeding program of the Antwerp Zoo and from commercial trade, respectively. The age of the specimens of *S. rostellatus* could not be deter-

mined properly. Because the standard length of the sectioned juvenile of *S. rostellatus* was not measured, the ratio head length over standard length of the other specimens was used to estimate the standard length by interpolation, resulting in a length of 13.1 mm (Table 1). All specimens were catalogued in the collection of the Zoological Museum of the Ghent University (UGMD).

The term juvenile instead of larva is conform with Balon (1975), because the fins are already differentiated. Newly released *H. kuda* resemble miniature adults and when they leave the pouch they are considered juveniles rather than larvae as in most marine teleosts (Choo and Liew, 2006). Besides that, growth allometries after release from the brood pouch reflect typical teleostean juvenile growth and not larval growth (Choo and Liew, 2006).

Adult as well as juvenile specimens of all species (with exception of a juvenile *H. reidi*) were cleared and stained with alizarin red S and alcian blue according to the protocol of Taylor and Van Dyke (1985). A stereoscopic microscope (Olympus SZX-7) equipped with a camera lucida was used to study and draw the bony and cartilaginous elements of the cranium. KOH 5% was used to completely disarticulate the suspensorium of an adult specimen of all species, so all bones could be individually examined in detail. In the juveniles, bone staining was not very clear, so serial histological cross-sections were used, which also enabled more precise detection of the skeletal elements. Prior to sectioning, specimens stored in ethanol 70% were decalcified with Decalc 25% (Histolab Products AB Gothenburg, Sweden), dehydrated through an alcohol series, and embedded in Technovit 7100 (Heraeus Kulzer Wehrheim, Germany). Semi-thin sections (5 µm) were cut using a sliding microtome equipped with a wolframcarbide coated knife (Leica Polycut SM 2500), stained with toluidine blue and mounted with DPX. Images of the sections were acquired using a digital camera (Colorview 8, Soft Imaging System) mounted on a light microscope (Polyvar, Reichert, Jung), controlled by the software program analySIS 5.0 (Soft Imaging System GmbH Münster, Germany). Graphical 3D-reconstructions of the chondrocranium of both *S. rostellatus* and *H. capensis* were generated, using Amira 3.1 (Template Graphics Software Mérignac, France) and Rhinoceros 3.0 software (McNeel Europe SL Barcelona, Spain). Sections were manually aligned, structures traced and surface models of the segmented structures were generated. The specimen of

S. rostellatus (13.1 mm SL) used for serial sectioning shows the hyoid in a resting position, whereas that of *H. capensis* (12.8 mm SL) has its hyoid depressed.

RESULTS

The terminology of the osteological components, for the most part, follows that of Lekander (1949) and Harrington (1955). The vomeral, circumorbital, parietal, and postparietal bones follow the terminology of Schultze (2008).

Juvenile cranium

Syngnathus rostellatus. The cartilaginous neurocranium consists of two parts which are separated by the eyes: the rostral ethmoid and the caudal otic capsule (see Fig. 1). The ethmoid plate is long and narrow but becomes wider rostrally where it lies ventral to the rostral cartilage (Fig. 1A,B). More caudally the ethmoid plate bears a vertical ridge, i.e., the internasal septum, connected to the orbitonasal laminae, which enclose the orbitonasal foramina (Fig. 1A,B). Although the ethmoid plate and the septum are firmly fixed, histological differences among the cartilaginous elements suggests that the internasal septum is not formed as an outgrowth of the ethmoid plate. There is a clear difference in the size, shape, and organization of their chondrocytes (Fig. 2D). The ethmoid plate is continuous with the trabecula communis, that lies medial to the orbits (Fig. 1B,C). Ventrally the otic capsule is provided with an articulation facet for the hyomandibular part of the hyosymplectic cartilage. Meckel's cartilage bears a ventral retroarticular process and articulates caudally with the pterygoquadrate part of the palatoquadrate cartilage, which is roughly L-shaped (Fig. 1A). The palatine part, which is completely separated from the pterygoquadrate part, lies lateral to the ethmoid plate (Fig. 1A). The largest cartilage element of the splanchnocranium is the hyosymplectic cartilage, which consists of a long, horizontal symplectic part, and a shorter oblique hyomandibular part (Fig. 1A,C). At the ventrocaudal margin of the hyosymplectic cartilage lies the interhyal cartilage, articulating ventrally with the ceratohyal cartilage (Fig. 1C). Medial of the two ceratohyal cartilages lies one long basihyal and two shorter hypohyal cartilages (Fig. 1C).

Juveniles of *S. rostellatus* show the onset of ossification in most places, however only a very thin layer of bone was observed (see Fig. 2). Ventral to the ethmoid plate the dermal parasphenoid bone has already formed. This very long bone runs from the ethmoid region up to the posterior part of the otic region (Fig. 2D,F). Formation of the mesethmoid bone begins dorsal to the ethmoid plate and around the internasal septum (Fig. 2C). A thin bony sheet at the ventral end of the orbitonasal

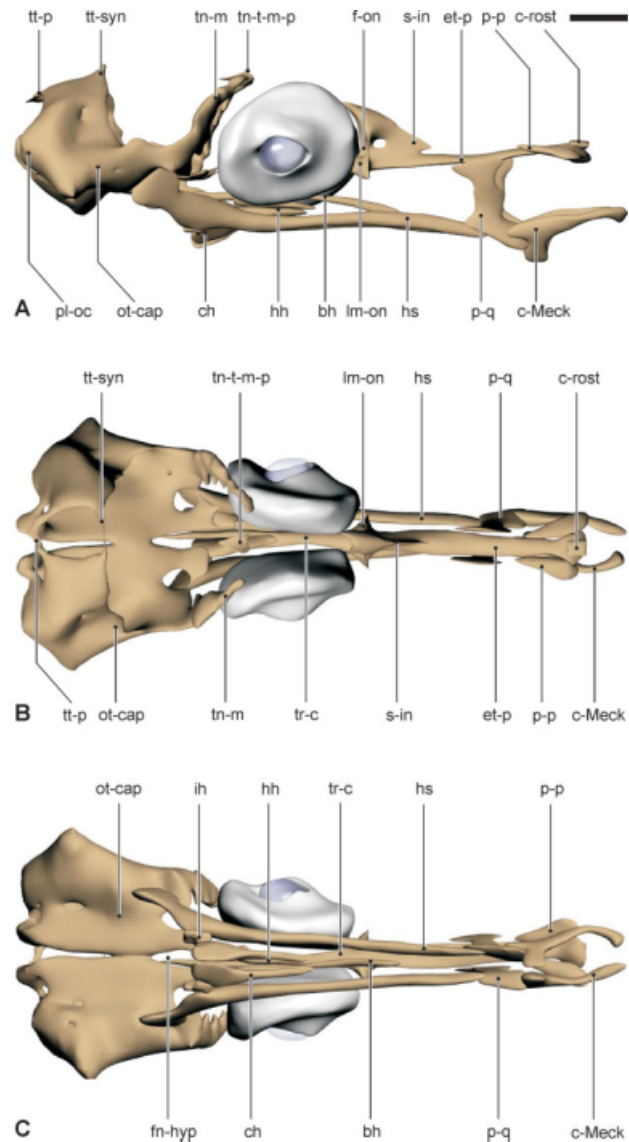


Fig. 1. 3D reconstruction of the juvenile chondrocranium of *Syngnathus rostellatus* UGMD175388 (13.1 mm SL). A lateral view of the right side; B dorsal view; C ventral view. Abbreviations: bh, basihyal cartilage; c-Meck, Meckel's cartilage; c-rost, rostral cartilage; ch, ceratohyal cartilage; et-p, ethmoid plate; f-on, orbitonasal foramen; fn-hyp, fenestra hypophyseae; hh, hypohyal cartilage; hs, hyosymplectic cartilage; ih, interhyal cartilage; lm-on, orbitonasal lamina; ot-cap, otic capsule; p-p, palatine part of palatoquadrate cartilage; p-q, pterygoquadrate part of palatoquadrate cartilage; ploc, pila occipitalis; s-in, internasal septum; tn-m, taenia marginalis; tn-t-m-p, taenia tecti medialis posterior; tr-c, trabecula communis; tt-p, tectum posterior; tt-syn, tectum synoticum. Scale bar, 0.2 mm.

laminae is the precursor of the lateral ethmoid bone. Around the main part of Meckel's cartilage, the dentary bone is formed (whether this bone includes the mentomeckelian and splenial bones is uncertain due to the absence of canals; Fig. 2B). This bone bears a large ventral ridge and posteriorly encloses the anguloarticular bone (this could

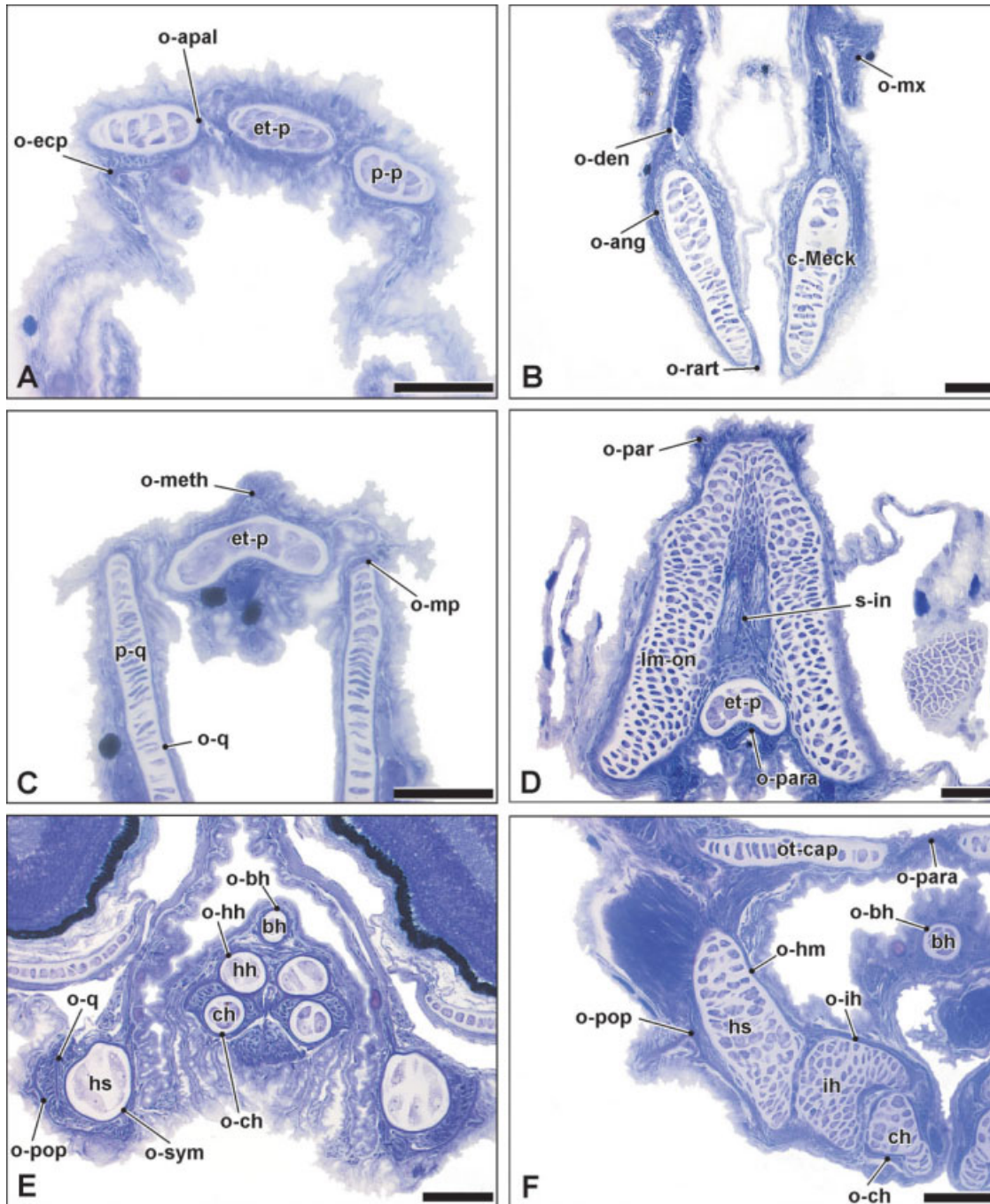


Fig. 2. Histological cross-sections of the juvenile cranium of *Syngnathus rostellatus* UGMD175388 (13.1 mm SL). A rostrorsal part of the snout at the level of the autopalatine; B lower jaw; C dorsal part of ethmoid region; D internasal region; E hyoid; F right hyoid-suspensorium articulation. Abbreviations: bh, basihyal cartilage; c-Meck, Meckel's cartilage; ch, ceratohyal cartilage; et-p, ethmoid plate; hh, hypohyal cartilage; hs, hyosymplectic cartilage; ih, interhyal cartilage; lm-on, orbitonasal lamina; o-ang, anguloarticular bone; o-apal, autopalatine bone; o-bh, basihyal bone; och, ceratohyal bone; o-den, dentary bone; o-ecp, ectopterygoid bone; o-hh, hypohyal bone; o-hm, hyomandibular bone; o-ih, interhyal bone; o-meth, mesethmoid bone; o-mp, metapterygoid bone; o-mx, maxillary bone; o-par, parietal bone; o-para, parasphenoid bone; o-pop, preopercular bone; o-q, quadrate bone; o-rart, retroarticular bone; o-sym, symplectic bone; ot-cap, otic capsule; p-p, palatine part of palatoquadrate cartilage; p-q, pterygoquadrate part of palatoquadrate cartilage; sin, internasal septum. Scale bars, 50 μ m.

be fused with the splenial bones, but again no canals were observed), which is still poorly developed and only present on the lateral side of Meck-

el's cartilage (Fig. 2B). The retroarticular bone is visible as a small ossification of the ventrocaudal part of the Meckel's cartilage (Fig. 2B). In the

upper jaw, both maxillary and premaxillary bones have appeared and are already fairly well developed. The former articulates with the rostral cartilage dorsally. The autopalatine bone is present but does not bear a clear maxillary or vomeral articulation facet yet (Fig. 2A). Ventral to the palatoquadrate cartilage the ectopterygoid bone is formed (Fig. 2A). This dermal bone shows a small horizontal part and a longer vertical one that meets the dorsal process of the quadrate bone. At the dorsal edge of the palatoquadrate cartilage, the small metapterygoid bone arises (Fig. 2C). The quadrate bone bears a dorsal process, as well as a ventromedial and ventrolateral wing. More caudally these wings enclose the cartilaginous hyosymplectic and the symplectic bone (Fig. 2C,E). The symplectic bone consists of both the ossification around the rostral part of the hyosymplectic cartilage and a dorsal crest on top of the perichondral part (Fig. 2E). The hyomandibular bone is formed caudally around the hyosymplectic cartilage and bears dorsal articulations with the neurocranium and opercular bone that remain cartilaginous (Fig. 2F). The preopercular bone consists of both a short and long process, the long one covers the quadrate and symplectic bones rostrally, and is also provided with a large lateral process (Fig. 2E). Its shorter oblique bar covers the hyomandibular bone caudally (Fig. 2F). All other elements of the hyoid arch, i.e., basihyal, hypohyals, ceratohyals, and interhyal cartilages, show the presence of a very thin sheet of bone (Fig. 2E,F). The hypohyal bones bear a ventrolateral and a ventromedial process, which surround the ceratohyal bones (Fig. 2E). Anterior and posterior ceratohyal bones are hard to distinguish from each other at this stage (Fig. 2E). Within the tendon of the sternohyoideus muscle, the urohyal bone has also arisen. The opercular bone is a thin but fairly large bony sheet, bearing a lateral process and articulating with the hyomandibular bone medially. None of the other opercular bones (interopercular, subopercular, and suprapreopercular bones) and neither the branchiostegal rays are present yet.

Hippocampus capensis

For the chondrocranium of *H. capensis* (see Fig. 3), we report only those features which differ from *S. rostellatus*.

The ethmoid plate of the cartilaginous neurocranium in *H. capensis*, is shorter and rostrally narrower than that of *S. rostellatus* (Fig. 3A,B). Caudal to the olfactory organs, the ethmoid plate widens and meets the orbitonasal laminae (Figs. 3A,B and 4D). It is also continuous with the trabecula communis, but in the seahorse the latter is much shorter and more robust (Fig. 3C). The otic capsule has a distinct position compared with that in *S. rostellatus*, namely dorsocaudally of the

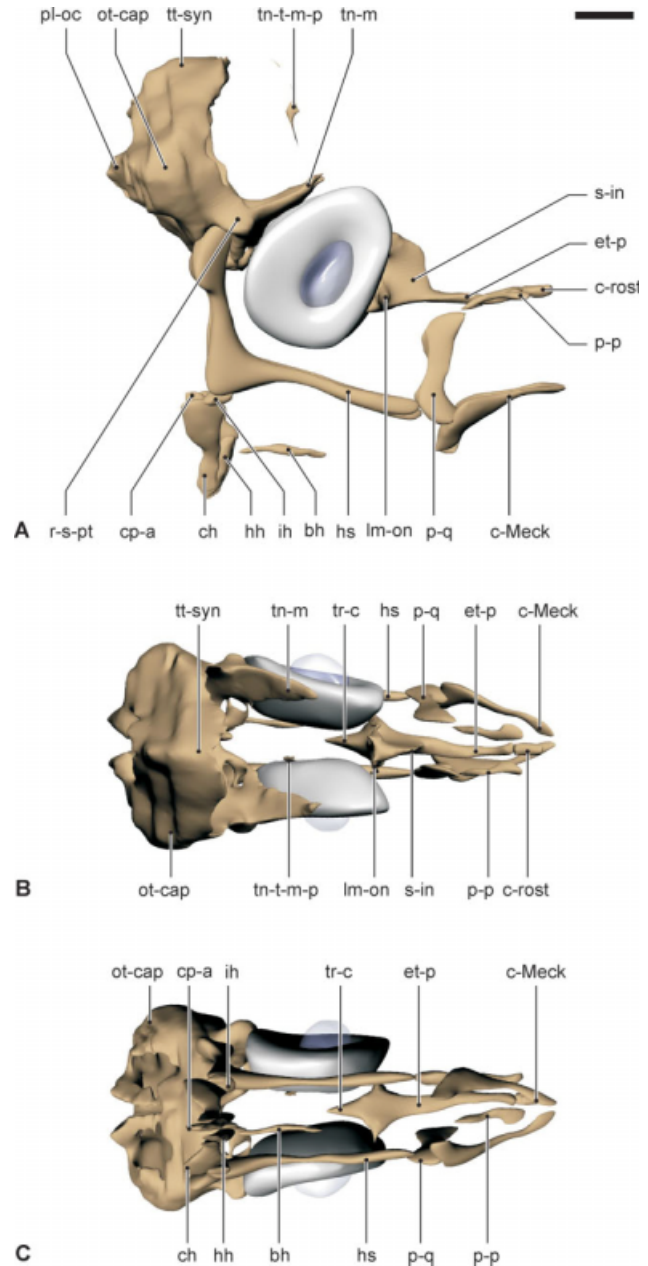


Fig. 3. 3D reconstruction of the juvenile chondrocranium of *Hippocampus capensis* UGMD175394 (12.8 mm SL) with hyoid depressed. A lateral view of the right side; B dorsal view; C ventral view. Abbreviations: bh, basihyal cartilage; c-Meck, Meckel's cartilage; c-rost, rostral cartilage; ch, ceratohyal cartilage; cp-a, anterior copula; et-p, ethmoid plate; hh, hypohyal cartilage; hs, hyosymplectic cartilage; ih, interhyal cartilage; lm-on, orbitonasal lamina; ot-cap, otic capsule; p-p, palatine part of palatoquadrate cartilage; p-q, pterygoquadrate part of palatoquadrate cartilage; ploc, pila occipitalis; r-s-pt, sphenopteroic ridge; s-in, internasal septum; tn-m, taenia marginalis; tn-t-m-p, taenia tecti medialis posterior; tr-c, trabecula communis; tt-syn, tectum synoticum. Scale bar, 0.2 mm.

orbits. Hence, it does not lie on the same level as the ethmoid plate, but at an angle to the latter (otic capsule tilted about 34° up; Fig. 3A). At the

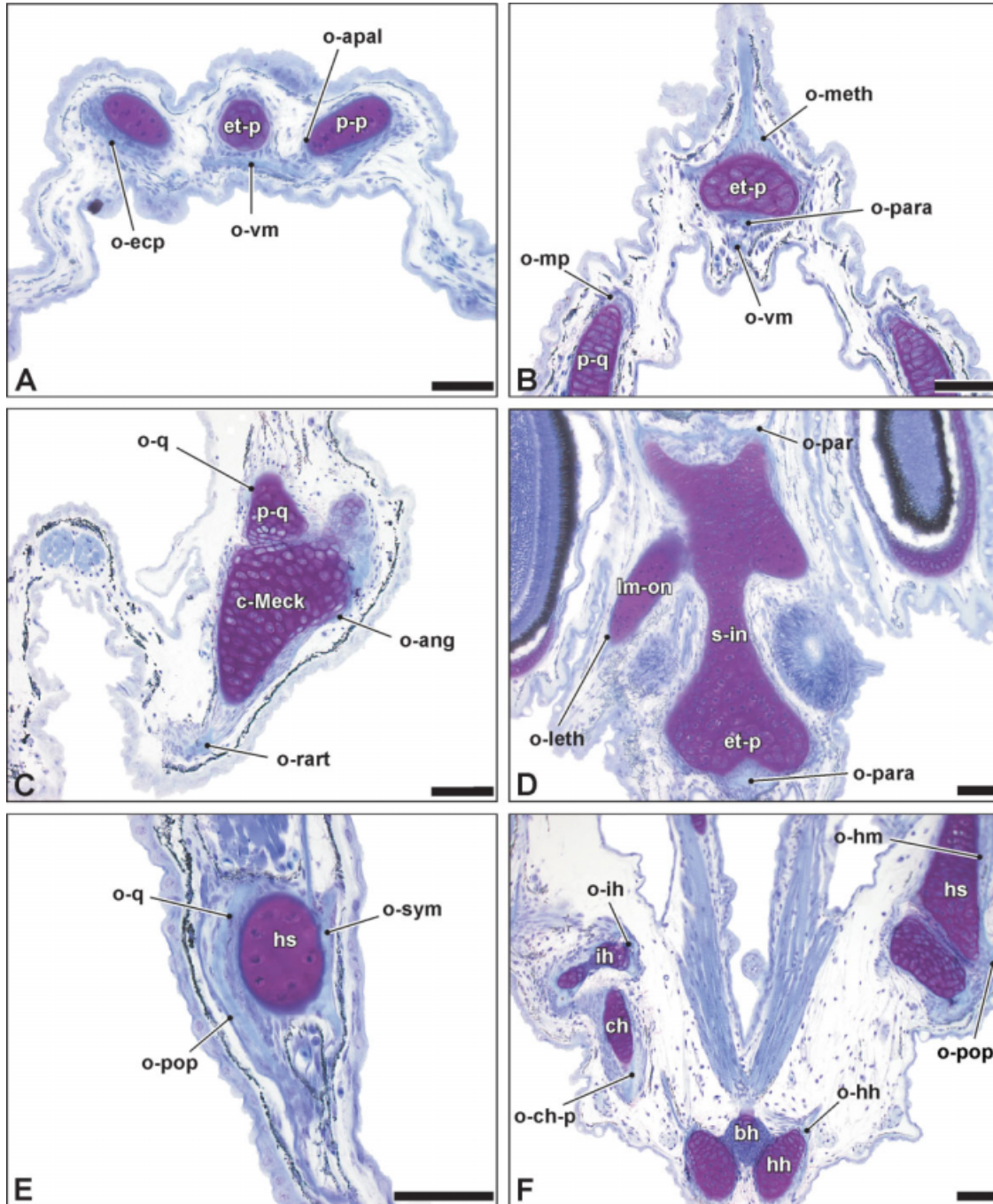


Fig. 4. Histological cross-sections of the juvenile cranium of *Hippocampus capensis* UGMD175394 (12.8 mm SL). A rostrorodorsal part of the snout at the level of the autopalatine; B dorsal part of ethmoid region; C left lower jaw; D internasal region; E part of right suspensorium; F hyoid-suspensorium articulation. Abbreviations: bh, basihyal cartilage; c-Meck, Meckel's cartilage; ch, ceratohyal cartilage; et-p, ethmoid plate; hh, hypohyal cartilage; hs, hyosymplectic cartilage; ih, interhyal cartilage; lm-on, orbitonasal lamina; o-ang, anguloarticular bone; o-apal, autopalatine bone; o-chp, posterior ceratohyal bone; o-ecp, ectopterygoid bone; o-hh, hypohyal bone; o-hm, hyomandibular bone; o-ih, interhyal bone; o-leth, lateral ethmoid bone; o-meth, mesethmoid bone; o-mp, metapterygoid bone; o-par, parietal bone; o-para, parasphenoid bone; o-pop, preopercular bone; o-q, quadrate bone; o-rart, retroarticular bone; o-sym, symplectic bone; o-vm, vomeral bone; p-p, palatine part of palatoquadrate cartilage; p-q, pterygoquadrate part of palatoquadrate cartilage; s-in, internasal septum. Scale bars, 50 μ m.

ventral surface of the otic capsule, the articulation facet of the hyomandibular part of the hyosymplectic cartilage is much more prominent and it is lat-

erally flanked by a spheno-pterotic ridge (Fig. 3A). The Meckel's cartilage is more tapered rostrally compared with that of *S. rostellatus* (Fig. 3A). The

symplectic part of the hyosymplectic cartilage is somewhat shorter in *H. capensis*. The hyomandibular part, however, is longer and more vertically orientated compared with that of the pipefish (Fig. 3A). In the seahorse, the shorter basihyal cartilage lies in front of the ceratohyal cartilages, which may be due to the hyoid being retracted (Fig. 3A,C).

Almost all bones are present in the juvenile *H. capensis* studied, except for the circumorbital bones (see Fig. 4). The vomeral bone lies ventral to the ethmoid plate and becomes covered by the parasphenoid bone more caudally (Fig. 4A,B,D). The latter bears two rather large lateral wings that reach the ventral surface of the otic capsule. The dentary bone rostrally bears a small lateral process and has a well developed coronoid process. The anguloarticular bone and retroarticular bone are prominent and there is a ligamentous connection between the retroarticular bone and the slender interopercular bone that continues to run up to the posterior ceratohyal bone (Fig. 4C). The dorsal crest of the symplectic bone is larger in *H. capensis* compared with *S. rostellatus* (Fig. 4E). There is a large spine on the lateral surface of the preopercular bone and the ascending bar is oriented vertically instead of obliquely as in the pipefish (Fig. 4F). The bony sheets around the hypohyal and ceratohyal cartilages are well developed (Fig. 4F). In addition, the anterior and posterior ceratohyal bones are distinct from each other. In the seahorse, the urohyal bone is much shorter. The opercular bone has a convex shape and bears a prominent lateral process. Also the subopercular bone and branchiostegal rays are fairly well developed in juvenile *H. capensis*.

Adult cranium

Syngnathus rostellatus. The most distinctive character of the skull of *Syngnathus rostellatus* is the highly extended tube snout (see Fig. 5). It is formed by the elongation of the vomeral, mesethmoid, and the circumorbital bones of the neurocranium and of the quadrate, metapterygoid, symplectic, preopercular, and interopercular bones of the splanchnocranium (Fig. 5A).

Both the maxillary and premaxillary bones are relatively small and toothless (Fig. 5A,B,D,E). The maxillary bone bears two cartilaginous processes dorsally: a rostral premaxillary one and a caudal one for the articulation with the vomeral bone. Below the latter process there is also a cartilaginous articulation surface for the autopalatine bone. The round rostral cartilage is situated medio-caudal of the maxillary bone and dorsally of the vomeral bone. Ventrally, the maxillary bone is triangularly shaped, covering the coronoid process of the dentary bone to which it is ligamentously connected. The slender premaxillary bone is

rostrocaudally flattened and tapers ventrally. It is provided with a dorsocaudal cartilaginous articulation head for the maxillary bone.

The vomeral bone is a long and narrow bone that broadens anteriorly, forming an articulation with the autopalatine bone laterally and the maxillary bone rostrally (Fig. 5A,B,D,E). The hind part of the vomeral bone reaches the lateral ethmoid bones and is covered dorsally by the mesethmoid bone. More caudally, it is wedged in a fissure of the parasphenoid bone. The mesethmoid bone covers more than half the length of the snout and stretches out caudally, up to the parietal bones (Fig. 5A,B). The lateral ethmoid bone is a slim bone that separates the nasal opening from the orbits (Fig. 5A,B).

The parasphenoid bone is positioned rostrally between the dorsal mesethmoid bone and the ventral vomeral bone (Fig. 5A). It bears two lateral wings behind the orbits and fits into a wedge of the basioccipital bone caudally. In most specimens studied of *S. rostellatus* only two circumorbital bones are present, which seem to be homologous to an antorbitolacrima and a second infraorbital bone (see discussion). Only one specimen has just one bone on its right side. In the individuals with two circumorbital bones, the large antorbitolacrima caudally reaches the front end of the nasal opening, and covers a large part of the quadrate bone (Fig. 5A,B). Ventrally, the antorbitolacrima shows one or several small indentations. The second infraorbital bone is much smaller and borders the ventral side of the nasal opening, as well as the anterior side of the orbits (Fig. 5A–C).

The large dentary bone of the lower jaw has a well developed coronoid process (Fig. 5A,C,D). Inside a cavity of the dentary bone, the smaller anguloarticular bone fits, which bears a distinctive cartilaginous articulation with the quadrate bone caudally (Fig. 5A,C,D). The retroarticular bone is very small, with a strong mandibulo-interopercle ligament connecting it to the interopercular bone (Fig. 5A,C,D).

In the adult stage, the autopalatine bone carries a prominent cartilaginous maxillary process, a smaller articulation condyle for the vomeral bone and a slender cartilaginous process caudally (Fig. 5A,B,D,E). There is no separate dermopalatine bone and as in most extant teleosts, it is probably fused to the autopalatine bone (Arratia and Schultze, 1991). The ectopterygoid bone is roughly triangularly shaped, with a vertical part running along the ascending process of the quadrate bone and a horizontal part that is covered dorsally by the vomeral bone (Fig. 5A,B,D,E). This dorsal part shows a gap into which the cartilaginous process of the autopalatine bone fits, with a firm connection linking both. Lateral to the vomeral bone and behind the ectopterygoid bone lies the metapterygoid bone which tapers posteriorly and is covered

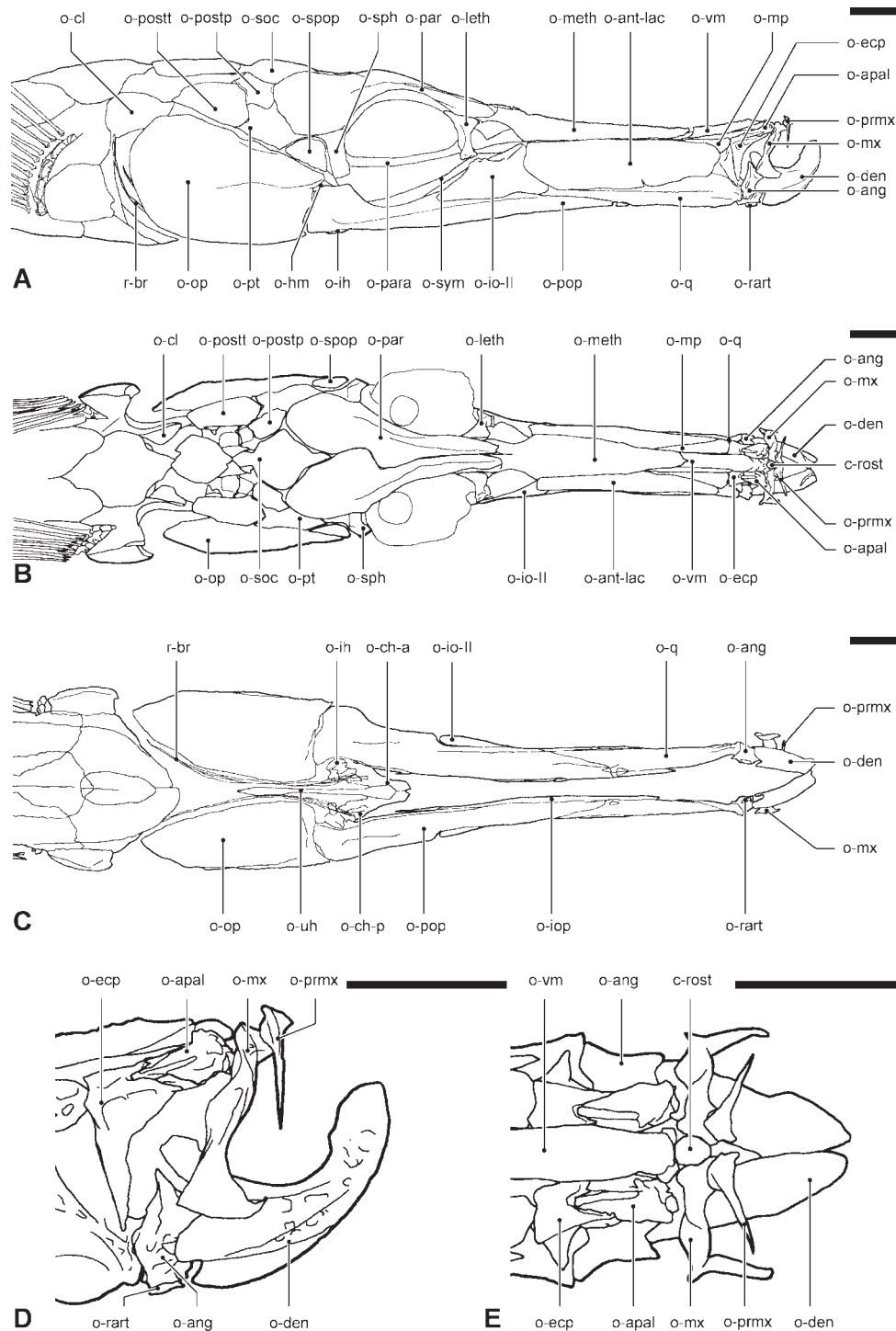


Fig. 5. Adult osteocranium of *Syngnathus rostellatus* UGMD175381 (111.1 mm SL). A lateral view of the right side; B dorsal view; C ventral view; D lateral view of snout tip; E dorsal view of snout tip. Abbreviations: c-rost, rostral cartilage; o-ang, angular-articular bone; o-ant-lac, antorbitolacrimal bone; o-apal, autopalatine bone; o-ch-a, anterior ceratohyal bone; o-ch-p, posterior ceratohyal bone; o-cl, cleithral bone; o-den, dentary bone; o-ecp, ectopterygoid bone; o-hm, hyomandibular bone; o-ih, interhyal bone; o-io-II, second infraorbital bone; o-iop, interopercular bone; o-leth, lateral ethmoid bone; o-meth, mesethmoid bone; o-mp, metapterygoid bone; o-mx, maxillary bone; o-op, opercular bone; o-par, parietal bone; o-para, parasphenoid bone; o-pop, preopercular bone; o-postp, postparietal bone; o-postt, posttemporal bone; o-prmx, premaxillary bone; o-pt, pterotic bone; o-q, quadrate bone; o-rart, retroarticular bone; o-soc, supraoccipital bone; o-sph, sphenotic bone; o-spop, suprapreopercular bone; o-sym, symplectic bone; o-uh, urohyal bone; ovm, vomeral bone; r-br, branchiostegal ray. Scale bars, 1 mm.

by the upper rostral margin of the lacrimal bone (Fig. 5A,B). The quadrate bone, a long perichondral bone that stretches out caudally, is mostly covered by the metapterygoid bone anteriorly and the two circumorbital bones posteriorly (Fig. 5A–C).

The hyomandibular bone articulates dorsally by a double condyle with the sphenotic and prootic bones, respectively, and bears a dorsocaudal opercular process. The symplectic bone is almost completely covered by the preopercular and circumorbital bones and forms the ventral border of the orbits (Fig. 5A). It bifurcates anteriorly into two processes: a lower horizontal part that joins the quadrate bone, and a more dorsal oblique crest lying behind the upper margin of the second infraorbital bone.

The long horizontal process of the preopercular bone overlaps with the quadrate bone anteriorly where it tapers (Fig. 5A,C). Medially, the preopercular bone has two ridges: one supporting the symplectic bone and one for insertion of the levator arcus palatini muscle, which continues to run along this ridge and more caudally in a groove of the hyomandibular bone. Ventrally the preopercular bone has a cartilaginous differentiation where the cartilaginous head of the interhyal bone articulates. There is no articulation between the interhyal bone and the hyomandibular bone. The interopercular bone is covered by the preopercular bone and the quadrate bone, with an interopercle-hyoid ligament connecting it to the posterior ceratohyal bone caudally (Fig. 5C). The interhyal bone, which is stout and small, is ventrally provided with a very firm, saddle-shaped joint for the posterior ceratohyal bone (Fig. 5A,C). The posterior ceratohyal bone has a small lateral process, close to the interhyal articulation (Fig. 5C). Onto this process, the interopercle-hyoid ligament attaches rostrally and at its caudal base, the two branchiostegal rays are connected. There is a firm interdigitation between the posterior and anterior ceratohyal bone. Distally, there is a small triangularly shaped gap between the left and right anterior ceratohyal bones, just below the very firm cartilaginous symphysis. The anterior ceratohyal bones are connected to the urohyal bone by a paired ceratohyal-urohyal ligament (Fig. 5C). The hypo-hyal bone is a small element that is firmly connected to the medial face of the anterior ceratohyal bone. Medial to the anterior ceratohyal bones and covered by the other elements of the hyoid lies the slender basihyal bone, which remains cartilaginous rostrally. The urohyal bone is a fairly long and slender bone that broadens somewhat rostrally where the ceratohyal-urohyal ligaments attach (Fig. 5C).

The opercular bone is large and has a convex lateral surface (Fig. 5A–C). There is just a tiny gill slit close to the cleithrum. The suprapreopercular

bone is a small bone lying dorsorostrally to the opercular bone (Fig. 5A,B). The subopercular bone is sickle shaped, covered by the ventral edge of the opercular bone. The two branchiostegal rays, which are long and slender, join the caudal margin of the opercular bone and reach up to the gill slit (Fig. 5A,C). There are no canals for the lateral line system present in any of the bones studied.

Hippocampus capensis

The premaxillary and maxillary bones look very similar to those in *S. rostellatus* (Fig. 6A,B,D,E). In *H. capensis*, however, they are more heavily built and the maxillary bone shows a more prominent convex curve when viewed rostrally. The rostral cartilage has a more elliptical shape instead of being round.

The dorsal part of the tube snout consists of the vomeral bone and the mesethmoid bone (Fig. 6B). The latter has a slightly bifurcated rostral end and covers approximately half the snout length. The lateral ethmoid bone is very distinct and has quite a large lateral process (Fig. 6A,B).

The parasphenoid bone stretches ventrally along the neurocranium and bends somewhat upward in the otic region (Fig. 6A). The number of circumorbital bones in *H. capensis* is variable. In spite of this variability, some of them can be considered as homologous (antorbital, lacrimal, and dermosphenotic bones) as indicated by Schultze (2008). The dermosphenotic bone is consistently present in all specimens observed. Variation was found at the level of all other circumorbital bones, including left right variation (e.g., one specimen, 97.6 mm SL, has an additional fourth circumorbital bone on its right side of which the homology is less obvious). Another specimen (99.0 mm SL) also seemed to have a fused antorbitolacrimal bone, whereas separate bones were observed in others. The most common pattern observed is where the antorbital bone is the smallest, covering the quadrate bone and the metapterygoid bone (Fig. 6A,B). The lacrimal bone also covers the quadrate bone and is provided with a dorsorostral gap into which the metapterygoid bone fits (Fig. 6A,B). Finally, the second infraorbital bone covers the quadrate, the preopercular and a large part of the symplectic bones (Fig. 6A–C). Of the circumorbital bones, the most anterior one covers the next at its caudal end, so the antorbital bone covers the lacrimal bone, which in turn covers the second infraorbital bone.

The dentary bone is a short but solid bone (Fig. 6A,C,D). Ventrocaudally, the anguloarticular bone bears two ventral processes in between which the small retroarticular bone fits (Fig. 6A,C,D).

The autopalatine bone is a rather slender bone whereas the ectopterygoid bone is somewhat firmer compared with the one in *S. rostellatus*

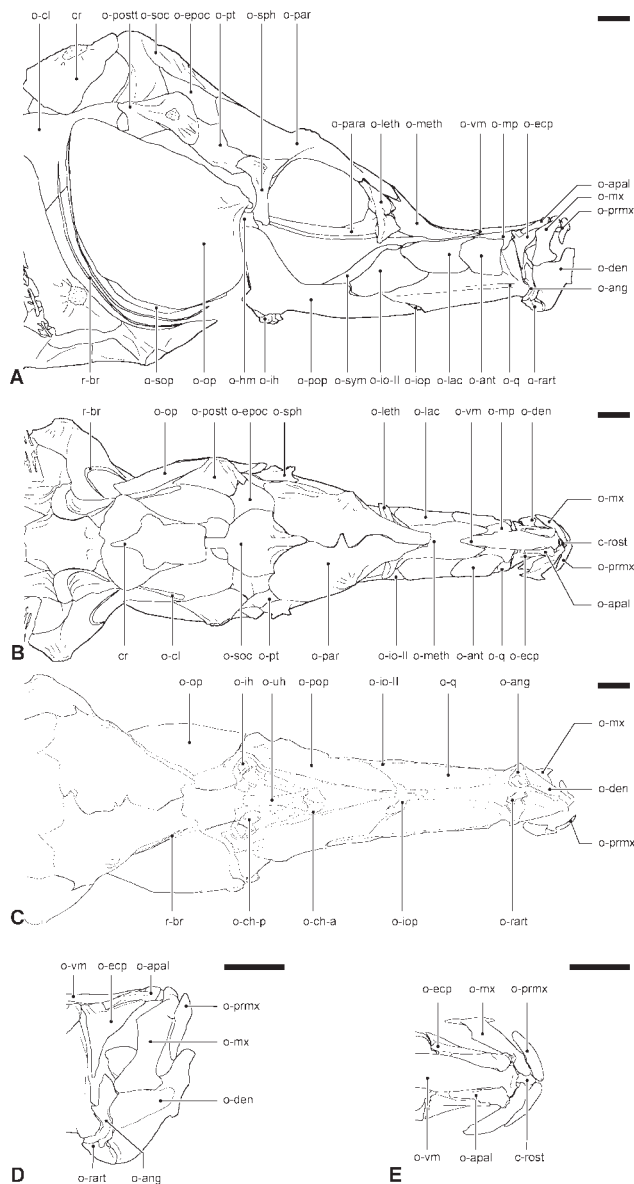


Fig. 6. Adult osteocranium of *Hippocampus capensis* UGMD175389 (96.1 mm SL). A lateral view of the right side; B dorsal view; C ventral view; D lateral view of snout tip; E dorsal view of snout tip. Abbreviations: c-rost, rostral cartilage; cr, corona; o-ang, anguloarticular bone; o-ant, antorbital bone; o-apal, autopalatine bone; o-ch-a, anterior ceratohyal bone; o-ch-p, posterior ceratohyal bone; o-cl, cleithral bone; o-den, dentary bone; o-ecp, ectopterygoid bone; o-epoc, epioccipital bone; o-hm, hyomandibular bone; o-ih, interhyal bone; o-io-II, second infraorbital bone; o-iop, interopercular bone; o-leth, lateral ethmoid bone; o-lac, lacrimal bone; o-meth, mesethmoid bone; o-mp, metapterygoid bone; o-mx, maxillary bone; o-op, opercular bone; o-par, parietal bone; o-para, parasphenoid bone; o-pop, preopercular bone; o-postt, posttemporal bone; o-prmx, premaxillary bone; o-pt, pterotic bone; o-q, quadrate bone; o-rart, retroarticular bone; o-soc, supraoccipital bone; o-sop, subopercular bone; o-sph, sphenotic bone; o-sym, symplectic bone; ouh, urohyal bone; o-vm, vomeral bone; r-br, branchiostegal ray. Scale bars, 1 mm.

(Fig. 6A,B,D,E). The metapterygoid bone fits into a gap of the lacrimal bone posteriorly (Fig. 6A,B).

The two neurocranial condyles of the hyomandibular bone are larger and more distant from each other in the seahorse. In addition, the hyomandibular bone is provided with a lateral process that is firmly connected to the preopercular bone. The oblique fork of the symplectic bone present in the pipefish is larger in the seahorse and forms a dorsal plate upon the perichondral part. Only the caudal part, that borders the ventrorostral margin of the orbits, is visible in a lateral view (Fig. 6A). The preopercular bone has a short ascending process that forms the posterior margin of the orbits (Fig. 6A,C). The interopercular bone is much shorter compared with that in *S. rostellatus* (Fig. 6A,C). The interhyal, the anterior and posterior ceratohyal, the hypohyal and basihyal bones resemble those of *S. rostellatus* (Fig. 6A,C). The urohyal bone, which is more robust, has a rostral bifurcation with both processes connected to the anterior ceratohyal bone by ceratohyal-urohyal ligaments (Fig. 6C).

The opercular bone is higher and has a less rounded dorsocaudal edge (Fig. 6A–C). The supraopercular bone is absent. The two very thin and slender branchiostegals reach up to the caudal edge of the opercular bone (Fig. 6A–C). As in *S. rostellatus* the canals for the lateral line are absent in all bones studied.

DISCUSSION

Bone terminologies

The dentary and anguloarticular bones in *Syngnathus rostellatus* and *Hippocampus capensis* could be a fusion of several bones. In most teleosts, the dentary bone comprises the perichondral mentomeckelian, the dermal splenial and the dermal dentary bones, and should thus be named “dento-splenio-mentomeckelium” according to the nomenclature of Lekander (1949). The anguloarticular bone is then the fusion of the perichondral articular bone, the dermal splenial bones and the dermal angular bone; the “angulo-splenio-articulare”. However, whether this is also the case for syngnathids is not certain, because the absence of the preoperculo-mandibular canal may indicate the absence of the splenial bones. In the current deficiency of conclusive ontogenetic evidence to elucidate this, the terms “dentary bone” and “anguloarticular bone” are used here.

Kindred (1924) suggested there is a pterygoid bone in *S. fuscus*, which would be a fusion of the ectopterygoid and the endopterygoid bones. According to Kadam (1961) the ectopterygoid and the endopterygoid bones ossify separately in *Nerophis* (species not stated), *S. serratus* and *Hippocampus* (species not stated). Bergert and Wainwright (1997) found both, an ectopterygoid

and an ectopterygoid bone, in *S. floridae*, and solely an ectopterygoid bone in *H. erectus*. In *S. rostellatus* and *H. capensis* we found no indications of an endopterygoid bone. As Kadam (1961) correctly pointed out, the bone that Kindred (1924) describes as the pterygoid bone consists as two separate elements and one of them is indeed the dermal ectopterygoid bone. However, he did not notice that the bone he called the endopterygoid bone is perichondral, and therefore homologous to a metapterygoid bone. Bergert and Wainwright (1997) followed Kindred (1924) in identifying the metapterygoid bone of *S. floridae* as the ectopterygoid bone. In addition, they did not mention the presence of a similar bone in *H. erectus*. Swinerton (1902) states that in *G. aculeatus* the pterygoid bone takes up the position of both ectopterygoid and endopterygoid bones, however, only one center of ossification is found. According to De Beer (1937) *Gasterosteus aculeatus* is in the possession of both an ectopterygoid and an endopterygoid bone, fused to form what he calls a pterygoid bone. We could not exclude a fusion between the ecto- and endo-ptyerygoid bone in *S. rostellatus* and *H. capensis*. However, based on its topography, ventrolateral to the autopalatine and the metapterygoid bone, this bone is considered homologous to the ectopterygoid bone.

As Branch (1966) mentioned, the homology of the circumorbital bones has been unclear. Kindred (1924), and De Beer (1937), defined the metapterygoid bone of *S. fuscus* as “the intramembranous ossification dorsal to the quadrate, rostral to the symplectic, and excluded from contact with the metapterygoid process of the palatoquadrate by the pterygoid”. However, Kadam (1961), Branch (1966), and Patterson (1977) pointed out this is not the metapterygoid bone, but the lacrimal bone. Jungersen (1910) identified the circumorbital bones as the posterior and anterior preorbital bones in *Syngnathus typhle* (which he called *Siphonostoma typhle*) because of their position lateral of the adductor mandibulae muscle. Gregory (1933) states that *Phyllopteryx* is in possession of “a row of antorbital plates on the side of the oral tube”, which he labels as two metapterygoid bones. As previously mentioned, Kindred (1924) and De Beer (1937) maintained that the lacrimal bone in *S. fuscus* is the metapterygoid bone, although they correctly pointed out that the second infraorbital bone is a circumorbital bone. Kadam (1961) described the two bones of the suborbital chain in *Nerophis* as an anterior preorbital bone and a posterior suborbital bone and he remarked that in *Syngnathus* and *Hippocampus* there are two preorbital bones. The use of the terms preorbital and suborbital bones should be avoided as they only indicate the position of these bones relative to the orbit but do not say anything about their homology (Daget, 1964). Therefore, we use the terms antor-

bita bone and infraorbital bones, as e.g., in Lekander (1949), Nelson (1969), and Schultze (2008). Occasionally, the term prevomer bone is used instead of vomer bone (Gregory, 1933; De Beer, 1937; Harrington, 1955), however because the homology with the vomer bone in sarcopterygians, the terminology of Schultze (2008) is followed here.

Aspects of snout elongation

As shown in Table 1, even though size ranges are similar, there is a difference in developmental stage between the juveniles of *Syngnathus rostellatus* (11.0–14.5 mm SL) and *Hippocampus capensis* (12.8–14.0 mm SL). Because of the different developmental stages of our specimens (*S. rostellatus* specimens had not left the brood pouch), we cannot link the morphological differences between the two species to differences in their developmental rate. However, this poses no problem for the main goal of this study, i.e., to show the relation between snout elongation and cranial morphology in an early developmental stage. Therefore, we will focus on the differences between both species, irrespective of their different developmental stages.

Both *S. rostellatus* and *H. capensis* have an elongated snout compared with *Gasterosteus aculeatus*. This elongation is restricted to the ethmoid region (vomer, mesethmoid, circumorbital, quadrate, metapterygoid, preopercular, interopercular, and symplectic bones). It appears to occur early in development, as observed in several Syngnathidae (e.g., *H. antiquorum* (Ryder, 1881), *S. peckianus* (McMurrich, 1883), *S. fuscus* (Kindred, 1921), *Hippocampus* (Kadam, 1958), and *Nerophis* (Kadam, 1961)). In *H. antiquorum* and *S. peckianus*, the ethmoid region is even elongated before the yolk sac is fully absorbed (Ryder, 1881; McMurrich, 1883).

A short comparison between some of these elements in syngnathids and the stickleback, as a generalized teleost representative without an elongated snout, is given here in order to understand the implications of snout elongation on cranial morphology in syngnathids (see Fig. 7).

The vomer bone stretches up to the lateral ethmoid bone in *S. rostellatus* and *H. capensis*, but in *Nerophis* it does not reach the nasal region (Kadam, 1961). According to Kadam (1961), this is a difference between the Gasterophori (syngnathids with the brood pouch rostral to anal fin: e.g., *Nerophis*) and the Urophori (brood pouch caudal to anal fin: e.g., *Syngnathus* and *Hippocampus*). Rostrally the vomer bone provides an articulation with the maxillary bone, but there is no mesethmoid-premaxilla articulation present as there is in primitive teleosts (Gregory, 1933).

In *S. rostellatus* and *H. capensis* the quadrate bone consists of a perichondral ascending process

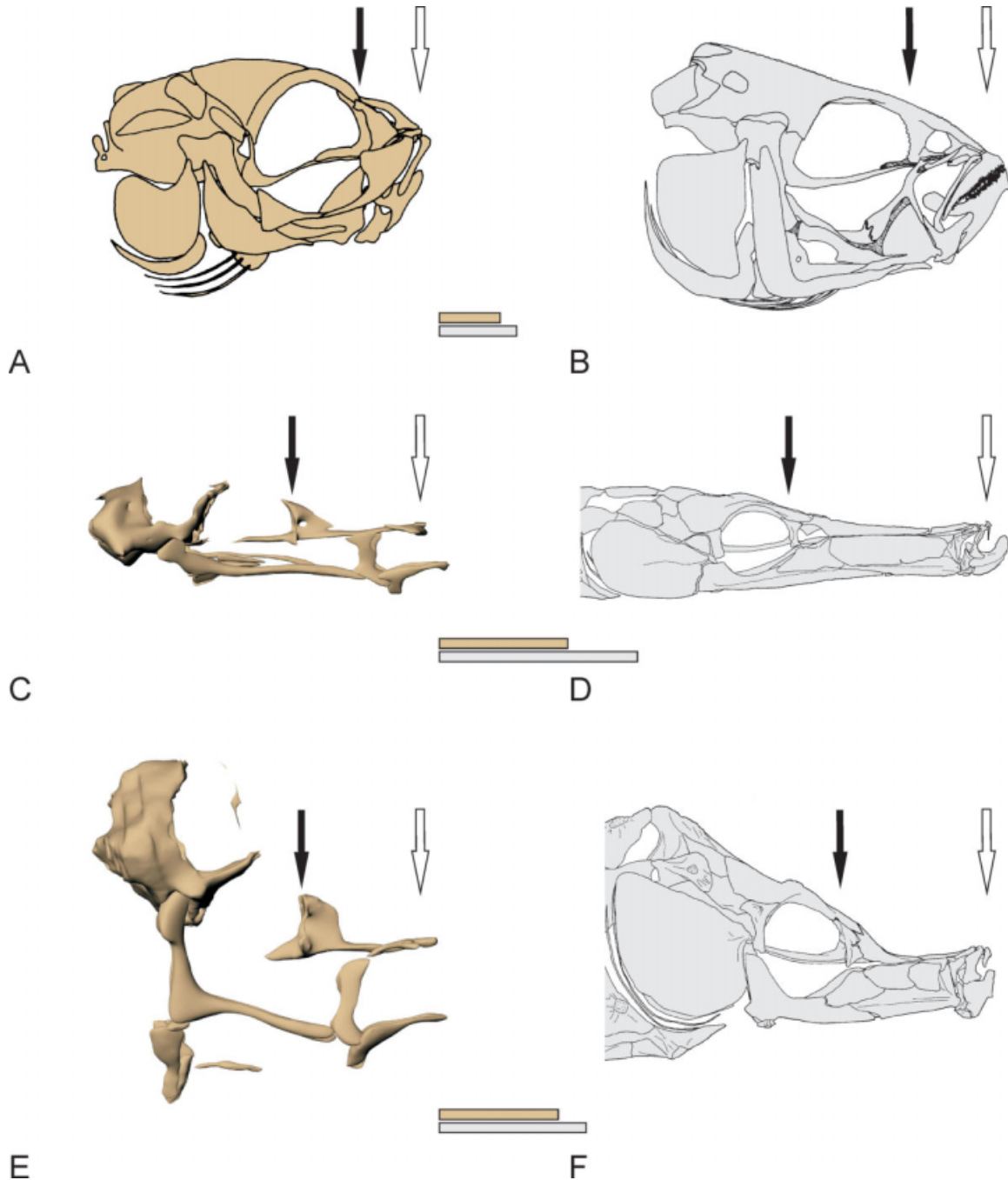


Fig. 7. Crania, scaled to same head length (from front of autopalatine bone to back of occipital region), of juveniles (beige) and adults (grey). A juvenile *G. aculeatus* (16.0 mm SL) (after Swinnerton, 1902); B adult *G. aculeatus* (SL not mentioned) (after Anker, 1974); C juvenile chondrocranium *S. rostellatus* UGMD175388 (13.1 mm SL); D adult *S. rostellatus* UGMD175381 (111.1 mm SL); E juvenile chondrocranium *H. capensis* UGMD175394 (12.8 mm SL); F adult *H. capensis* UGMD175389 (96.1 mm SL). Black arrows indicates rostral border of orbita, white arrows indicate front of the autopalatine bone. Area in between the arrows corresponds to the ethmoid region. Bars show length of ethmoid region relative to head length of juveniles (beige) and adults (grey). Note the elongation in both syngnathid species.

and a membranous horizontal process. Whether or not this horizontal process is homologous to the one considered a teleostean synapomorphy by Arratia and Schultze (1991), could not be confirmed here. The process is much smaller on the

quadrate bone in *G. aculeatus*, which is triangularly shaped with its apex dorsally (Anker, 1974). The ventrorostral corner of the quadrate bone provides the articulation with the lower jaw and ventrocaudally it bears a cartilaginous extension

that lies lateral to the symplectic bone (Anker, 1974).

The preopercular bone in *S. rostellatus* and *H. capensis* is L shaped. In the former the horizontal process is substantially longer than the vertical one, while in *H. capensis* the difference is less and in *G. aculeatus* the vertical process is the largest (Anker, 1974). Caudally, this vertical process meets the opercular bone in syngnathid species (Jungersen, 1910; Kindred, 1924; Kadam, 1961; Branch, 1966), but in *G. aculeatus* they only join each other dorsally (ventrally they are separated by an ascending process of the subopercular bone; Swinnerton, 1902; Anker, 1974).

In *G. aculeatus* the interopercular bone covers the subopercular bone caudally (Anker, 1974), but both lie well separated from each other in *S. rostellatus* and *H. capensis*.

The occurrence of an antorbital bone and lacrimal bone, followed by six infraorbital bones bordering the orbit (the first, third, and sixth being the lacrimal, jugal, and dermosphenotic bones, respectively), is a primitive feature of most teleosts (Reno, 1966; Nelson, 1969; Schultze, 2008). In the suborder Syngnathoidei other circumorbital bones besides the lacrimal bone are usually absent (Nelson, 2006), however, in syngnathids there are usually two to three infraorbital bones, which develop late (Kadam, 1961). In *S. rostellatus* and *H. capensis* the circumorbital bones are positioned in front of the orbit instead of around it. There is, however, a difference between those two species, as most specimens of the seahorse studied have an antorbital bone, a lacrimal bone (= first infraorbital bone) and a second infraorbital bone, whereas there are only two circumorbital bones present in almost all *S. rostellatus* specimens studied. Here, the posterior one corresponds to the second infraorbital bone. The anterior one is the largest one and appears to be a fusion between the antorbital bone and the lacrimal bone. This hypothesis is supported by the absence of a separate antorbital bone, the bone being as large as and taking the place of both the antorbital bone and the lacrimal bone in *H. capensis*. In addition, there is a ventral indentation that could point out the incomplete fusion between the antorbital bone and the lacrimal bone. The formation of the antorbitolacrimal bone could be a structural advantage to strengthen the elongated snout laterally. During the fast elevation of the snout, large, ventrally oriented forces are expected to be exerted onto the dorsal part of the snout. In the case of an unfused antorbital bone and lacrimal bone, a possible bending zone between the two bones exists. The formation of an antorbitolacrimal bone could reduce the risk of bending and still allows lateral expansion of the snout. In *G. aculeatus* there are three separate circumorbital bones present (Swinnerton, 1902; De Beer, 1937; Anker, 1974).

Fast suction feeding adaptations

Syngnathid fishes are known to capture prey by an unusual feeding strategy known as pipette feeding (de Lussanet and Muller 2007). They perform a rapid elevation of the head, which brings the mouth quickly close to the prey (Muller 1987). Then, expansion of their long snout generates a fast water flow that carries the prey into the mouth. This increase in buccal volume is mainly achieved by a lateral expansion, instead of ventral expansion typical for most suction feeding fish (Roos et al., in press). The hyoid is known to play an important role in suspensorium abduction as well as in depression of the lower jaw (Roos et al., in press).

Seahorses and pipefishes are ambush predators, they sit and wait until a prey comes close to the mouth (Foster and Vincent, 2004). They are known to consume mainly small crustaceans such as amphipods and copepods (Foster and Vincent, 2004; Kendrick and Hyndes, 2005) and a recent study by Castro et al. (2008) showed that nematodes are also one of the main food items consumed in the wild. According to Kendrick and Hyndes (2005) the trophic specialization of these fishes can be explained by their extreme snout morphology (length and gape), their feeding behavior and in the case of seahorses, their low mobility.

Syngnathids have a very small mouth aperture, severely limiting food particle size. The maxillary and premaxillary bones of *S. rostellatus* and *H. capensis* are rather small. Teeth, both oral, and pharyngeal, are absent and prey is swallowed whole (Lourie et al., 1999). *Gasterosteus aculeatus*, however, has a large, teeth bearing, premaxillary bone that is protrusible (De Beer, 1937; Alexander, 1967a; Anker, 1974; Motta, 1984; Nelson, 2006). Under the condition that a long ascending process of the premaxillary bone can be associated with a great amount of protrusion (Gosline, 1981; Motta, 1984; Westneat and Wainwright, 1989; Westneat, 2004), the lack of an ascending process in *S. rostellatus* and *H. capensis* indicates there is no upper jaw protrusion (Branch, 1966; Bergert and Wainwright, 1997). They do have a small rostral cartilage, rostrorodorsally of the ethmoid plate and medially of the maxillary bones. This is not necessarily an adaptation to the powerful suction feeding but could rather be an ancestral feature also found in Percidae, Cichlidae, Atherinoidei, Gasterosteidae and others, where it assists in upper jaw protrusion (Alexander and Mc, 1967a,b; Motta, 1984). Alternatively, the rostral cartilage in syngnathids could be involved in the fast rotation of the maxillary and premaxillary bones during mouth opening. Depression of the lower jaw induces a rostral swing of the maxillary bone, because of the firm primordial ligament running from the coronoid process to the maxillary bone. As a conse-

quence of the connection between maxillary and premaxillary bones, both rotate anteriorly. The mouth aperture is then laterally enclosed, resulting in a more circular gape, hence, a more anteriorly directed water flow into the mouth might be generated as hypothesized by Lauder (1979; 1985) and experimentally shown by Sanford et al. (2009). Kindred (1921) and Kadam (1961) also found a rostral cartilage in *S. fuscus* and *Nerophis*, which is connected to the palatine cartilage with dense connective tissue. Kadam (1958) further mentions a rostral cartilage articulating with the premaxillary and maxillary bones in *Hippocampus*.

The lower jaw of *S. rostellatus* and *H. capensis* is similar to the one in *G. aculeatus*, but much shorter relative to their head length. The anguloarticular bone in the syngnathid species is more tightly fixed to the dentary bone, improving the rigidity of the lower jaw. This might facilitate abduction of the left and right lower jaws, observed during manipulation of specimens (Roos et al., in press). In the stickleback there is no fusion between the angular bone and articular bone. The angular bone also fits into a cavity of the dentary bone, but with a potential pivoting zone in between them (Anker, 1974). There is a saddle-like joint between the articular bone and the quadrate bone, as in *S. rostellatus* and *H. capensis*.

The metapterygoid bone is a perichondral ossification of the metapterygoid process of the palatoquadrate cartilage (Arratia and Schultze, 1991). In *G. aculeatus*, as in other general teleosts, the quadrate and the hyomandibular bones are connected by means of the metapterygoid bone, forming the suspensorium (Gregory, 1933; Anker, 1974). This is not the case in *S. rostellatus* and *H. capensis*, where there is no connection between the short metapterygoid and the hyomandibular bones. Neither is there a connection between the very rudimentary metapterygoid process of the pterygoquadrate part of the palatoquadrate cartilage and the hyosymplectic cartilage in the pipefish and seahorse juveniles.

The symplectic part of the hyosymplectic cartilage in *S. rostellatus* juveniles is very long compared with the hyomandibular part, with the angle between these two parts being obtuse. In *H. capensis*, both parts are almost equally long and they are perpendicular to each other. This arrangement looks very much like the one in *G. aculeatus* (Swinnerton, 1902; Kindred, 1924). Kadam (1961) describes the symplectic bone in *Nerophis* as a chondromembranous bone with a perichondral part, namely the ossification of the anterior region of the hyosymplectic cartilage, and an intramembranous part, which rises up from the perichondral part. The vertical plate bears a dorsorostral process and decreases gradually in height more caudally. This is also found in *S. rostellatus* and *H. capensis*.

At the 6.3–9.0 mm SL stage of *G. aculeatus*, where there is no ossification of the cranial cartilage yet, the hyomandibular part of the hyosymplectic cartilage already has the two-headed articulation with the neurocranium as seen in adults (Swinnerton, 1902; Kindred, 1924; De Beer, 1937; Anker, 1974). The dorsorostral condyle articulates in a socket formed by the sphenotic bone, the dorsocaudal condyle fits in a socket of the pterotic bone (Anker, 1974). In the juvenile syngnathids (*S. rostellatus*, *H. capensis*, and *H. reidi*), there is only a single cartilaginous articulation. The hyomandibular bone in adult *S. rostellatus* and *H. capensis* is similar to the one in *G. aculeatus*; it also bears a double articular facet with the neurocranium, as in *H. reidi*. Dissection and manipulation of this double hyomandibular articulation in *S. rostellatus* and *H. capensis* proved that it is very firm. Strikingly, in *S. fuscus* (Kindred, 1924; De Beer, 1937), *Nerophis* (Kadam, 1961) and *S. acus* (Branch, 1966) only a single condyle is present, which is thought to increase the freedom of movement of the hyomandibular bone (Kindred, 1924; Branch, 1966).

The connection between the suspensorium and the hyoid arch is provided by the interhyal bone. The general teleost articulation is a ball-and-socket joint, with a rod-shaped interhyal bone bearing a rounded head that fits into a facet of the suspensorium, allowing the interhyal bone to rotate in every direction with respect to the suspensorium (Anker, 1989; Aerts, 1991). The configuration in *G. aculeatus* is comparable (Anker, 1974). This is not true for *S. rostellatus* and *H. capensis*, where the interhyal bone articulates with the preopercular bone dorsally and bears two articulation heads ventrally, in between which the posterior ceratohyal bone articulates. In that way, movement is more restricted to one in a rostrocaudal direction, resulting in a hyoid retraction during the expansive phase of the suction feeding. The two heads of the hyomandibular bone in combination with the robust interhyal bone can be assumed to indirectly reduce the degrees of freedom between the hyoid and the neurocranium, hence contraction of the sternohyoideus muscle is expected to be translated in a more powerful hyoid depression. Fast hyoid rotation is thus possible with a reduced risk of disarticulation of the ceratohyal bone. In *S. peckianus* (McMurrich, 1883), *S. fuscus* (De Beer, 1937), *Nerophis* (Kadam, 1961), *S. acus* (Branch, 1966), *S. floridae* and *H. erectus* (Bergert and Wainwright, 1997) the interhyal bone is similar, but it is claimed to articulate with the hyomandibular bone instead of the preopercular bone.

Muller and Osse (1984) showed that high negative pressures will be reached in the gill cavity of the pipefish *Entelurus aequoreus* during prey capture. According to Osse and Muller (1980) the

small gill slit and the strongly ossified gill cover are considered adaptations to the pipette type of feeding, characterized by a very fast neurocranial elevation (Muller and Osse, 1984; Muller, 1987; de Lussanet and Muller, 2007). The pressure in the opercular cavities is considered to be higher with increasing snout length, and a comparison between different syngnathid species showed that increasing snout length also results in a structurally more robust opercular bone (e.g., more ridges, greater curvature and thicker; Osse and Muller, 1980; Muller and Osse, 1984). In both, *S. rostellatus* and *H. capensis*, the gill slits are nearly closed by a firm sheet of connective tissue covered with skin. Only at the dorsocaudal tip a small aperture is left. Their opercular bone is firm and thick and has a convex surface which will help in withstanding medially directed forces. Comparison between the two species reveals that the opercular bone in the pipefish, which has a more elongated snout, is smaller, thicker and has a greater curvature, as expected.

The branchiostegal rays support the branchiostegal membrane, which closes the gill cavity ventrally. Among teleosts there can be more than 20 branchiostegal rays, but acanthopterygians almost never have more than eight (Gosline, 1967; Arratia and Schultze, 1990). In syngnathids the number of branchiostegal rays varies between one and three (McAllister, 1968). Here, in *S. rostellatus* and *H. capensis*, there are only two branchiostegal rays present on each side. As Gosline (1967) pointed out, the number of branchiostegal rays is related to the length of the hyoid bar. In syngnathids, the hyoid is relatively small, which might be associated with its lost function as a mouth bottom depressor (Roos et al., in press). A longer hyoid will have an increased moment of inertia resulting in hyoid depression at a lower velocity. In addition, the angle between the working line of the sternohyoideus muscle and the hyoid will become less favorable as the hyoid length increases. Thus, the length of the hyoid bar is expected to be constrained and consequently, there will be less available space for attachment of the branchiostegal rays.

In both adult and juvenile *H. capensis* the braincase is tilted dorsally with respect to the ethmoid region so it is situated dorsocaudally to the orbita instead of caudally as in *S. rostellatus*, *S. fuscus* and *Nerophis* (all pipefishes; Kindred, 1921; Kadam, 1961). In the *H. reidi* juvenile (7.01 mm SL) this dorsal tilting of the otic capsule was also visible, although the tilt was less than the one in *H. capensis* juvenile (only about 20° up compared with 34° in the latter). In adult *H. capensis*, more or less the same tilt is observed (38° up). Kadam (1958) described the presence of a sphenopterotic ridge at the base of the taeniae marginales (which he calls postorbital processes) in *Hippocampus*,

that appears to be missing in *Nerophis* (Kadam, 1961) and *S. fuscus* (Kindred, 1921). We also observed this ridge in *H. capensis* and *H. reidi*, but not in *S. rostellatus*. Apart from that, the hyosymplectic articulation socket medio-caudal to this ridge, is more distinct in the *Hippocampus* species studied.

It is obvious that already at an early developmental age, the juvenile feeding apparatus resembles that of adult *S. rostellatus* and *H. capensis*. This might be the result of the specialized parental care that enables the postponing of release from the brooding pouch until an advanced developmental state is reached. In the seahorse brooding pouch, oxygen is supplied through surrounding capillaries and the male prolactin hormone is secreted, inducing breakdown of the chorion to produce a placental fluid (Lourie et al., 1999; Carcupino et al., 2002; Foster and Vincent, 2004). Lack of oxygen and endogenous energy is probably not longer a limiting factor and emergence from the pouch may be delayed, as in *Galeichthys feliceps*, an ariid mouth-brooder (Tilney and Hecht, 1993).

ACKNOWLEDGMENTS

Research was supported by FWO grant G 053907. H.L. is funded by a PhD grant of the Institute for the Promotion of Innovation through Science and Technology in Flanders (IWT-Vlaanderen).

LITERATURE CITED

- Aerts P. 1991. Hyoid morphology and movements relative to abducting forces during feeding in *Astatotilapia elegans* (Teleostei: Cichlidae). *J Morphol* 208:323–345.
- Alexander R, Mc N. 1967a. The functions and mechanisms of the protrusible upper jaws of some acanthopterygians fish. *J Zool Lond* 151:43–64.
- Alexander R, Mc N. 1967b. Mechanisms of the jaws of some atheriniform fish. *J Zool Lond* 151:233–255.
- Anker GCh. 1974. Morphology and kinetics of the head of the stickleback, *Gasterosteus aculeatus*. *Trans Zool Soc Lond* 32:311–416.
- Anker GCh. 1989. The morphology of joints and ligaments of a generalised *Haplochromis* species: *H. elegans* Trewavas 1933 (Teleostei, Cichlidae). III. The hyoid and the branchiostegal apparatus, the branchial apparatus and the shoulder girdle apparatus. *Neth J Zool* 39:1–40.
- Arratia G, Schultze HP. 1990. The urohyal: Development and homology within Osteichthyan. *J Morphol* 203:247–282.
- Arratia G, Schultze HP. 1991. Palatoquadrate and its ossifications: Development and homology within Osteichthyan. *J Morphol* 208:1–81.
- Balon EK. 1975. Terminology of intervals in fish development. *J Fish Res Board Can* 32:1663–1670.
- Bergert BA, Wainwright PC. 1997. Morphology and kinematics of prey capture in the syngnathid fishes *Hippocampus erectus* and *Syngnathus floridae*. *Mar Biol* 127:563–570.
- Branch GM. 1966. Contributions to the functional morphology of fishes. Part III. The feeding mechanism of *Syngnathus acus* Linnaeus. *Zool Afr* 2:69–89.

- Carcupino M, Baldacci A, Mazzini M, Franzoi P. 2002. Functional significance of the male brood pouch in the reproductive strategies of pipefishes and seahorses: A morphological and ultrastructural comparative study on three anatomically different pouches. *J Fish Biol* 61:1465–1480.
- Castro ALD, Diniz AD, Martins IZ, Vendel AL, de Oliveira TPR, Rosa IMD. 2008. Assessing diet composition of seahorses in the wild using a non destructive method: *Hippocampus reidi* (Teleostei: Syngnathidae) as a study-case. *Neotrop Ichthyol* 6:637–644.
- Choo CK, Liew HC. 2006. Morphological development and allometric growth patterns in the juvenile seahorse *Hippocampus kuda* Bleeker. *J Fish Biol* 69:426–445.
- Daget J. 1964. Le crane des téléostéens. *Mém Mus Natn Hist Nat série A* 31:163–341.
- de Lussanet MHE, Muller M. 2007. The smaller your mouth, the longer your snout: Predicting the snout length of *Syngnathus acus*. *Centriscus scutatus* and other pipette feeders. *J R Soc Interface* 4:561–573.
- De Beer GR. 1937. The development of the vertebrate skull. Oxford: Clarendon Press. p. 552.
- Foster SJ, Vincent ACJ. 2004. Life history and ecology of seahorses: Implications for conservation and management. *J Fish Biol* 64:1–61.
- Gosline WA. 1967. Reduction in branchiostegal ray number. *Copeia* 1:237–239.
- Gosline WA. 1981. The evolution of the premaxillary protrusion system in some teleostean fish groups. *J Zool* 193:11–23.
- Gregory WK. 1933. Fish skulls: a study of the evolution of natural mechanisms. *Trans Am Phil Soc* 23:75–481.
- Harrington RW. 1955. The osteocranium of the American cyprinid fish, *Notropis bifrenatus*, with an annotated synonymy of teleost skull bones. *Copeia* 4:267–291.
- Jungersen HFE. 1910. Ichthyotomical contributions. II. The structure of the *Aulostomidae*, *Syngnathidae* and *Solenostomidae*. *Dansk vidensk Naturv* 8:267–364.
- Kadam KM. 1958. The development of the chondrocranium in the seahorse *Hippocampus (Lophobranchii)*. *J Linn Soc Zool* 43:557–573.
- Kadam KM. 1961. The development of the skull in *Nerophis (Lophobranchii)*. *Acta Zool-Stockholm* 42:1–42.
- Kendrick AJ, Hyndes GA. 2005. Variations in the dietary compositions of morphologically diverse syngnathid fishes. *Environ Biol Fishes* 72:415–427.
- Kindred JE. 1921. The chondrocranium of *Syngnathus fuscus*. *J Morphol* 35:425–456.
- Kindred JE. 1924. An intermediate stage in the development of the skull of *Syngnathus fuscus*. *Am J Anat* 33:421–447.
- Lauder GV. 1979. Feeding mechanics in primitive teleosts and in the halecomorph fish *Amia calva*. *J Zool Lond* 187:543–578.
- Lauder GV. 1985. Aquatic feeding in lower vertebrates. In: Hildebrand M, Bramble DM, Liem KF, Wake DB, editors. *Functional Vertebrate Morphology*. Cambridge: The Belknap Press. pp. 210–229.
- Lekander B. 1949. The sensory line system and the canal bones in the head of some Ostariophysi. *Acta Zool-Stockholm* 30:1–131.
- Lourie SA, Vincent ACJ, Hall HJ. 1999. Seahorses: An identification guide to the world's species and their conservation. London: Project Seahorse. p. 214.
- McAllister DE. 1968. The evolution of branchiostegals and associated opercular, gular, and hyoid bones and the classification of teleostome fishes, living and fossil. *Bull Natl Mus Can (Biol Ser)* 221:1–239.
- McMurrich MA. 1883. On the osteology and development of *Syngnathus peckianus* (Storer). *Q J Microsc Sci* 23:623–650.
- Motta PJ. 1984. Mechanics and function of jaw protrusion in teleost fishes: A review. *Copeia* 1:1–18.
- Muller M. 1987. Optimization principles applied to the mechanism of neurocranium levation and mouth bottom depression in bony fishes (Halecostomi). *J Theor Biol* 126:343–368.
- Muller M, Osse JWM. 1984. Hydrodynamics of suction feeding in fish. *Trans zool Soc Lond* 37:51–135.
- Nelson GJ. 1969. Infraorbital bones and their bearing on the phylogeny and geography of osteoglossomorph fishes. *Am Mus Novita* 2394:1–37.
- Nelson JS. 2006. *Fishes of the world*. New Jersey: John Wiley & Sons. p. 601.
- Osse JWM, Muller M. 1980. A model of suction feeding in teleostean fishes. In: Ali MA, editor. *Environmental Physiology of Fishes*. New York: Plenum Publishing Corporation. pp. 335–352.
- Patterson C. 1977. Cartilage bones, dermal bones and membrane bones, or the exoskeleton versus the endoskeleton. In: Andrews SM, Miles RS, Walker AD, editors. *Problems in Vertebrate Evolution*. London: Academic Press. pp. 77–121.
- Reno HW. 1966. The infraorbital canal, its lateral-line ossicles and neuromasts, in the minnows *Notropis volucellus* and *N. buchanani*. *Copeia* 3:403–413.
- Roos G, Leysen H, Van Wassenbergh S, Herrel A, Jacobs P, Dierick M, Aerts P, Adriaens D. 2009. Linking morphology and motion: A test of a four-bar mechanism in seahorses. *Physiol Biochem Zool* 82:7–19.
- Roos G, Van Wassenbergh S, Herrel A, Aerts P. Kinematics of suction feeding in the seahorse *Hippocampus reidi*. *J Exp Biol* (in press).
- Ryder JA. 1881. A contribution to the development and morphology of the Lophobranchiates (*Hippocampus antiquorum*, the sea-horse). *Bull U S Fish Comm* 1:191–199.
- Sanford CPJ, Day S, Kinow N. 2009. The role of mouth shape on the hydrodynamics of suction feeding in fishes. *Integr Comp Biol* 49 (Suppl. 1):e149.
- Schultze HP. 2008. Nomenclature and homologization of cranial bones in actinopterygians. In: Arratia G, Schultze HP, Wilson MVH, editors. *Mesozoic fishes 4 - Homology and Phylogeny*. München: Verlag Dr. Friedrich Pfeil. pp. 23–48.
- Swinerton HH. 1902. A contribution to the morphology of the teleostean head skeleton, based upon a study of developing skull of the three-spined stickleback (*Gasterosteus aculeatus*). *Q J Microsc Sci* 45:503–597.
- Taylor WR, Van Dyke GC. 1985. Revised procedures for staining and clearing small fishes and other vertebrates for bone and cartilage study. *Cybium* 9:107–119.
- Tilney RL, Hecht T. 1993. Early ontogeny of Galeichthys feliceps from the south east coast of South Africa. *J Fish Biol* 43:183–212.
- Van Wassenbergh S, Roos G, Genbrugge A, Leysen H, Aerts P, Adriaens D, Herrel A. 2009. Suction is kid's play: Extremely fast suction in newborn seahorses. *Biol Lett* 5:200–203.
- Westneat MW. 2004. Evolution of levers and linkages in the feeding mechanisms of fishes. *Integr Comp Biol* 44:378–389.
- Westneat MW, Wainwright PC. 1989. Feeding mechanism of *Epibulus insidiator* (Labridae; Teleostei): evolution of a novel functional system. *J Morphol* 202:129–150.